The role of charge in the toxicity of polymer-coated cerium oxide nanomaterials to *Caenorhabditis elegans*

Devrah A. Arndt[a], Emily K. Oostveen[a], Judy Triplett[b], D. Allan Butterfield[b], Olga V. Tsyusko[a], Blanche E. Collin [c], Daniel L. Starnes [a], Jian Cai[d], Jon B. Klein[d,] Richard Nass[e], and Jason M. Unrine[a]

a) Department of Plant and Soil Sciences, University of Kentucky, Lexington, Kentucky, United States

b) Department of Chemistry, University of Kentucky, Lexington 40506, United States

c) CNRS, IRD, Coll. France, CEREGE, Aix Marseille Université, Aix-en-Provence, France

d) Center for Proteomics, University of Louisville, Louisville, KY 40202

e) Department of Pharmacology and Toxicology, Indiana University, Indianapolis, Indiana 46202, United States

Correspondence addressed to Jason Unrine, jason.unrine@uky.edu;

Abstract:

This study examined the impact of surface functionalization and charge on ceria nanomaterial toxicity to *Caenorhabditis elegans*. The examined endpoints included mortality, reproduction, protein expression, and protein oxidation profiles. *Caenorhabditis elegans* were exposed to identical 2-5 nm ceria nanomaterial cores which were coated with cationic (diethylaminoethyl dextran; DEAE), anionic (carboxymethyl dextran; CM), and non-ionic (dextran; DEX) polymers. Mortality and reproductive toxicity of DEAE-CeO_2 was approximately an order of magnitude higher than for CM-CeO_2 or DEX-CeO_2. Two-dimensional gel electrophoresis with orbitrap mass spectrometry identification revealed changes in the expression profiles of several mitochondrial-related proteins and proteins that are expressed in the *C. elegans* intestine. However, each type of CeO_2 material exhibited a distinct protein expression profile. Increases in protein carbonyls and protein-bound 3-nitrotyrosine were also observed for some proteins, indicating oxidative and nitrosative damage. Taken together the results indicate that the magnitude of toxicity and toxicity pathways vary greatly due to surface functionalization of CeO_2 nanomaterials.

KEYWORDS: ceria nanoparticle, nanotoxicology, proteomics, oxidative stress, surface charge

1. Introduction

CeO$_2$ engineered nanomaterials (CeO$_2$-ENMs) are valued for their catalytic properties, and they are used as diesel fuel additives, chemical/mechanical planarization agents in glass and semiconductor production, and in energy storage devices (Pirmohamed et al., 2010; Ranga, 2003; Steele, 1999; Steele and Heinzel, 2001). CeO$_2$-ENMs are also being explored for use in medical applications as therapeutic antioxidants (Chigurupati et al., 2013; Ciofani et al., 2014). The manufacture, consumption, and disposal of these products can result in the release of CeO$_2$-ENMs to the environment through wastewater effluent, sewage sludge biosolids, or atmospheric fallout of diesel particulates, with soils and sediments expected to be the ultimate sink in the environment (Collin et al., 2014a).

Caenorhabditis elegans has emerged as a key model organism for ecotoxicity studies and nanotoxicity studies alike (Choi et al., 2014). *C. elegans* are a useful tool for toxicology research because their genome is fully sequenced, mapped and annotated, and it has a sizable suite of functional genomic tools, including large numbers of mutant and transgenic strains, and facile knockdown of gene expression through RNAi (Brenner, 1974; Costanzo et al., 2000; Leung et al., 2008). In a previous study, *C. elegans* exhibited decreased reproduction after exposure to 1 mg Ce/L CeO$_2$-ENMs with diameters of 15 and 45 nm (Roh et al., 2010). In contrast, decreased lifespan was observed in *C. elegans* after exposure to a far lower concentration of 0.14 μg Ce/L with diameters of 8.5 nm (Zhang et al., 2011). A key difference between these studies was the surface chemistry of the CeO$_2$-ENMs. The former study investigated uncoated particles while the latter study used particles coated with hexamethyleneteramine. The toxicity of

5

hexamethylenteramine (HMT) alone was not evaluated by Zhang et al., and it is possible that this coating is toxic by itself. Alternatively, it could be that differences in the surface chemistry of the particles themselves caused the dramatic differences in toxicity between these two studies.

Studies in other model organisms provide evidence that surface charge is a key factor determining toxicity of CeO_2-ENMs. Cationic CeO_2-ENMs coated with aminated polyacrylic acid exhibited greater cytotoxicity to A549 and MCF-7 cancer cell lines than anionic polyacrylic acid-coated or non-ionic dextran-coated CeO_2-ENMs (Asati et al., 2010), although comparison of the non-ionic CeO_2-ENMs is somewhat complicated by the fact that its polymer coating was different than for the cationic and anionic materials and that the CeO_2 cores themselves were prepared using different methods. Our previous work indicated that toxicity and biotransformation of CeO-ENMs are dramatically altered by the charge of polymer surface coatings. (Collin et al., 2014b). That same study demonstrated that Ce was partially reduced from Ce (IV) to Ce (III) in vivo and that the degree of reduction also depended on polymer surface coating charge. The increased toxicity associated with the cationic CeO_2-ENMs could be explained by increased electrostatic attraction to biological membranes as compared to negatively-charged particles (Chen et al., 2009; Goodman et al., 2004; Wang et al., 2012) and differences in subcellular distribution (Asati et al., 2010).

Oxidative stress often results from CeO_2-ENM exposure, and has been observed in a variety of organisms including *C. elegans, Pseudokirchneriella subcapitata, Daphnia magna, Danio rerio,* Sprague Dawley rats*,* and Fisher rats (Rogers et al., 2015) (Hardas et al., 2012; Park et al., 2008; Van Hoecke et al., 2009; Yokel et al., 2009). However, the

specific role of CeO_2-ENM surface charge on toxicity pathways and patterns of oxidative damage to biomolecules has not been well explored. Based on the influence of surface charge on subcellular distribution observed by Asati et al. (2010) and the oxidation state of CeO_2 particles observed by Collin et al. (2014b), we hypothesize that exposure to CeO_2-ENMs with different surface charges will result in distinct patterns of protein expression and oxidative damage to proteins.

To test our hypotheses, we used 2-4 nm CeO_2-ENMs coated with 10 kDa dextran and functionalized them with either diethylaminoethyl groups to yield positively charged particles or carboxymethyl groups to yield negatively charged particles. The advantage of this approach is that identical cores are used and the polymer used to coat the surface differs only by substitution of hydroxyl groups with functional groups that confer a net negative or net positive charge over a wide pH range. Mortality and reproduction were measured as lethal and sub-lethal endpoints of toxicity for this study, and expression and redox proteomics were utilized to investigate patterns of protein expression and oxidative damage.

2. Materials and methods

2.1 CeO$_2$ nanomaterial synthesis and characterization. The synthesis and characterization of the test materials has been previously described (Collin et al., 2014b). CeO_2-ENMs (2-4 nm diameter) were first coated with 10 kDa dextran (DEX-CeO_2). Dextran is not ionized at circumneutral pH and since the pH of zero net charge (PZC) of CeO_2 is near 7, the particles have a zeta potential close to zero (Collin et al., 2014b). DEX-CeO_2 particles were subsequently functionalized with diethylaminoethyl groups to

yield cationic particles (DEAE-CeO$_2$) or carboxymethyl groups to yield anionic particles (CM-CeO$_2$).

Primary particle diameter was determined by transmission electron microscopy (TEM) (JOEL 2010 F microscope; Tokyo, Japan). A NanoZS 90 Malvern Zetasizer (Malvern, United Kingdom) was used to measure hydrodynamic diameter (by dynamic light scattering; DLS) and electrophoretic mobility (by phase analysis light scattering; PALS) of CeO$_2$-ENMs in *C. elegans* exposure media (moderately hard reconstituted water; MHRW (USEPA, 2002)). The Hückel approximation was used to estimate zeta potential from electrophoretic mobility of the particles. Verification of the expected functionalization of the coatings was performed using Fourier transform infrared spectroscopy (FTIR). The FTIR results are reported by Collin et al. (2014b). Ceria suspensions were acid digested following US EPA method 3015 (spectrometry, 1998) and concentration was measured by inductively coupled plasma mass spectrometry (ICP-MS) (Agilent 7500cx, Santa Clara, CA).

2.2 Mortality. *Caenorhabditis elegans* (Wild type, N2 Bristol Strain) were obtained from the Caenorhabditis Genetics Center (Minneapolis, MN) and age synchronization was performed according to previously established methods (Donkin and Williams, 1995; Materials), 2012). Nine to eleven L3-stage nematodes were exposed to one mL of CeO$_2$-ENMs (0-5,000 mg Ce/L) for 24 hours with feeding (10 μL/mL *E. coli;* OP50 strain) or 1 mL of CeO$_2$-ENMs (0-5,000 mg Ce/L) without feeding. *C. elegans* were counted as dead if unresponsive to a gentle prodding (Williams and Dusenbery, 1990). Percent mortality was compared between controls and treatments using Bonferroni-corrected two-tailed t-tests ($\alpha = 0.05$). For this and the reproduction assay discussed below, concentrations

were selected to attempt to obtain a full concentration response curve. These concentraitons probably exceed what is expected in the natural environment by a large margin (Collin et al., 2014a), but they may be relevant to exposures where CeO2 is used as a drug. Comparision of the effects of surface coating requires that full concentration-response curves be determined.

2.3 *Reproduction*. L2-stage nematodes were exposed to CeO_2-ENMs for 48 hours with feeding using *E.coli* OP_{50} strain at the rate of 10 μL/mL and $OD_{600} = 1$ for the stock solution. The exposures were conducted in moderately hard reconstituted water (USEPA, 2002) and the exposure medium and food were refreshed at 24 hours. After the exposure, individual nematodes were placed on 6 cm K-agar plates (Williams and Dusenbery, 1988) seeded with *E. coli* OP_{50} and allowed to lay eggs for 48 hours before transfer to a new K-agar plates. This was repeated thrice. After removing the adult nematode, juveniles were stained with 0.5 mg/L rose bengal (0.5 mg/L) (Acros Organics, New Jersey, USA) and heat killed for one hour at $50^{o}C$ prior to counting offspring. Nematodes were counted as viable if they were fully emerged from the egg cuticle. Each CeO_2-ENM concentration was replicated five or six times. Reproduction was quantified by counting the total number of offspring per nematode and controls and treatments were compared using two-tailed Bonferroni corrected *t*-tests (α = 0.05).

2.4 Protein expression and redox proteomics.

Stage L1 *nematodes* were exposed for 48 hours in six mL of CeO_2-ENM at concentrations that corresponded to the EC30 for reproduction for each particle type as determined in the previously described assays (500 mg/L DEX-CeO_2, 750 mg/L CM-CeO_2, and 3.25 mg/L DEAE-CeO_2). The EC30 for reproduction was chosen so that the

nematodes would be exposed to equitoxic concentrations of the materials. Therefore, differences in proteomic responses can be interpreted as differences in mechanisms of toxicity and not differences in degree of toxicity. After the 48-hour exposure period, nematodes were transferred to K-agar plates to grow for an additional 24 hours to increase the amount of protein available for extraction. For protein extraction, 200 to 300 nematodes were suspended in 0.5 mL sucrose isolation buffer (0.32 M sucrose, 2 mM EDTA, 2 mM EGTA, 20 mM HEPES) with a protease inhibitor cocktail (104 mM 4-(2-Aminoethyl) benzenesulfonyl fluoride hydrochloride, 80 µM aprotinin, 4 mM bestatin, 1.4 mM E-64, 2 mM leupeptin, 1.5 mM pepstatin A). The nematode pellet was frozen at -80°C and then thawed in an ice bath and ultrasonicated with a Misonix Ultrasonic Liquid Processor (Misonix, Inc., New York, USA) using the microtip for two 10 second intervals at 30% amplitude. Protein concentration was determined using a BCA Protein Assay Reagent kit (Pierce Protein Biology Products, Rockford, IL). Extracted proteins were stored at -80° C.

2.4.1 Slot Blots. The slot blot technique (Bio-Dot SF apparatus, Bio-Rad Laboratories, Eugene, OR) was used to investigate changes in concentrations of three major markers of oxidative damage: protein carbonyls, protein-bound 3-nitrotyrosine (3NT), and protein-bound 4-hydroxy-2-nonenal (HNE). For protein carbonyls, samples were derivatized with 2,4-dinitrophenylhydrazine (DNPH) for recognition by a primary antibody as previously described (Sultana and Butterfield, 2008). Proteins were bound to nitrocellulose membranes (0.2 µm, Bio-Rad) and incubated with primary antibodies for derivatized protein carbonyls, 3-NT, and HNE. The following antibodies were used: Rb x dinitrophenol (EMD Millipore, Billerica, MA) diluted 1:1,000, anti-nitrotyrosine (Sigma

Aldrich, St. Louis. MO) diluted 1:10,000, anti-HNE (Alpha Diagnostics International, San Antonio, TX) diluted 1:10,000. Membranes were then washed three times with wash blot (0.2% w/v Tween 20 and 0.01% w/v sodium azide dissolved in PBS), incubated for one hour with anti-rabbit IgG alkaline phosphatase secondary antibody diluted to 1:10,000, developed with BCIP/NBT enzyme conjugates, and scanned into the ChemiDoc MP System with ImageLab software (Bio-Rad). Technical replicates (individual blots) were averaged for each biological replicate and n corresponds to the number of independent biological replicates. Normalized data from slot blots were evaluated with analysis of variance (ANOVA) followed by Tukey's test ($\alpha = 0.05$). Normality and homoscedasticity assumptions were tested using Shapiro-Wilk's and Bartlett's tests, respectively.

2.4.2 Protein expression by two-dimensional gel electrophoresis. Extracted protein (150 µg) was precipitated with trichloroacetic acid and shaken for 90 minutes with 200 uL rehydration buffer (8M urea, 2M thiourea, 2.0 % (w/v) CHAPS, 50 mM DTT, 0.2% biolytes, 0.01% Bromophenol Blue). Samples were placed on ReadyStrip IPG strips pH 3-10 (BioRad) and actively rehydrated (20 °C for 18 hours at 50 V) and isoelectrically focused (300 V for two hours, 500 V for two hours, 1,000 V for two hours, 8,000 V for eight hours) in a Protean Isoelectric Focusing (IEF) instrument (BioRad). For phase two separation, IPG strips were incubated for 10 minutes in the dark with equilibration buffer A (6M urea, 2% (w/v) SDS, 0.375M Tris-HCl (pH 8.8), 20% (v/v) glycerol, and 0.5% DTT), and 10 minutes in the dark with equilibration buffer B (6M urea, 2% (w/v) SDS, 0.375M Tris-HCl (pH 8.8), 20% (v/v) glycerol, and 4.5% IA). IPG strips were rinsed with TGS running buffer and placed in linear gradient (8-16%) Tris-HCl polyacrylamide

11

gels, 11 cm IPG/prep+1 well (Biorad) for gel electrophoresis (200 V for 65 minutes). Gels were fixed (10% acetic acid and 50% methanol) for one hour and stained with SYPRO ruby for 21 hours for protein detection.

2.4.3 Western blotting for detection of protein carbonyls, 3-NT, and HNE. Proteins were transferred to 0.2 µm nitrocellulose membranes in a Trans-blot Turbo Blotting instrument (BioRad). Membranes were blocked overnight in 3% BSA and incubated with primary antibody (Rb x dinitrophenyl diluted 1:1,000; anti-3-NT diluted 1:10,000; and anti-HNE diluted 1:10,000) for two hours (blots developed for protein carbonyls were first derivatized with DNPH before blocking). Membranes were washed three times in wash blot (5 min each) and incubated for one hour with secondary antibody (1:10,000 anti-rabbit IgG alkaline phosphatase for colorimetric development or 1:10,000 horseradish peroxidase for chemiluminescent development). Membranes were washed three more times in wash blot (5 min, 10 min, 10 min) and developed by colorimetric methods (BCIP/NBT solution) or by chemiluminescent methods with a Clarity Western ECL substrate kit (Biorad, Hercules, CA).

2.4.4 Image Analysis. SYPRO ruby and western blot images were captured using ImageLab software and analyzed by PDQuest 2D Analysis software (Biorad). For expression proteomics, the SYPRO ruby gels were matched to a master gel, and spot intensities for SYPRO ruby stained gels were quantified by densitometry in PDQuest. Individual gel intensities were normalized to the total density of each gel. The spot fluorescence intensities were compared between control spots and treatment spots and statistical significance was determined using two-tailed t-tests ($\alpha = 0.05$). For redox proteomics, two master gels were chosen (the master gel from the SYPRO ruby stained

gel set and a master gel from the oxidative marker western blot set), matched, and analyzed in PDQuest. Spot optical densities from the protein western blots were normalized to the SYPRO ruby spot fluorescence intensities, followed by comparison of values between controls and treatments. This procedure was repeated for western blots developed for protein carbonyl, 3-NT, and HNE.

2.4.5 Trypsin digestion and peptide extraction. Spots that exhibited statistically significant differences from controls in PDQuest were chosen for trypsin digestion, peptide extraction, analysis by nanoLC-orbitrap-MS/MS. Methods for peptide extraction, trypsin digestion, and identification by nanoLC-orbitrap-MS/MS have been previously described (Triplett et al., 2015).

2.5 Experimental validation. A subset of proteins/genes that were significantly different from controls in PDQuest and identified by nanoLC-orbitrap-MS/MS were chosen for experimental validation. We took a multifaceted approach to validation, taking advantage of traditional methods as well as functional genomics tools available for *C. elegans*. Validation procedures included 1D gel verification, Q-RT-PCR, *C. elegans* mutant reproduction assay, *C. elegans* GFP strain fluorescence assay, and immunoprecipitation.

2.5.1 *1D western blots*. Protein (25 µg) was added to sample buffer (6.8 pH 0.5 M Tris, 40% glycerol, 8% SDS, 20% β-mercaptoethanol, 0.01% Bromophenol Blue), heated for five minutes at 95 °C, and cooled on ice. Samples were loaded onto 12% Criterion TGX stain-free gels (Biorad) in MOPS buffer. Gels were run for 15 minutes at 80 V and 90 minutes at 120 V, scanned with a BioRad ChemiDoc XRS+ imaging system, transferred to nitrocellulose membranes (0.2 µm), and developed for the protein of interest as described in section 2.4.3. Bands in the western blot were normalized to the total protein

in the 1D gel. Treatments values were compared to controls with *t*-tests (α = 0.10). We accepted a higher probability of a type one error for this tests because we could only perform a small number of replicates.

2.5.2 *Verification by Quantitative Real Time Polymerase Chain Reaction (qRT-PCR)*.

Caenorhabditis elegans (N2 strain) were exposed as described in section 2.4.0. RNA was extracted with Trizol, treated with DNase and cleaned up with the RNeasy kit (Qiagen). After extraction and clean up, 150 ng RNA/sample was converted into cDNA with a High Capacity RNA-to-cDNA Kit by (Applied Biosystems). cDNA was added to TaqMan fast advanced master mix and TaqMan gene assay containing relevant primers and probes in a volume of 10 μL. The amplification reactions were performed in triplicates on StepOnePlus Real-Time PCR System (Applied Biosystems) following 10 min at 95°C, and 40 cycles of 10 s at 95°C and 30 s at 60°C. Negative controls and minus reverse transcription (−RT) negative controls were included for every gene/sample to check for DNA contamination. Among the genes selected for the verification were two heat shock proteins (*hsp-1* and *hsp-6*) and enolase (*enol-1*). We used TaqMan primer-probe sets for this. The assay IDs and primer effeciencies for these primer-probe sets are Ce02469085_g1(92.6%) for *hsp-1*, Ce02474686_g1 (109.2%) for *hsp-6*, and Ce02421723_g1 (107.3%) for *enol-1*. The reference gene used for normalization, Y45F10D.4 (ID = Ce02467252_g1, effeciency = 99.8%), has been previously described (Zhang et al., 2012), and its expression did not vary among significantly treatments as confirmed by qRT-PCR. qRT-PCR data were analyzed using the Relative Expression Software Tool (REST) (Pfaffl et al., 2002). Statistical significance was determined using REST at α = 0.05.

2.5.3 *Verification with mutant reproduction assay*. Mutants for *unc-15* (strain CB-1215) were acquired from the Caenorhabditis Genetics Center and exposed as described in section 2.4.0. After the 48-hour exposure, a reproduction assay was performed as described in section 2.3. Significance was determined using *t*-tests (α = 0.05) comparing number offspring between mutant and wild-type.

2.5.4   *Verification with fluorescence assay using GFP strain*. A green fluorescent protein (GFP) transgenic fusion strain for *hsp-6*, *hsp6::gfp* (zcIs13)*,* was acquired from the Caenorhabditis Genetics Center and exposed as described in section 2.4.0. GFP fluorescence was analyzed with an epifluorescence microscope (Nikon, Eclipse 90i, Tokyo, Japan) at 40X magnification at 24 hr, and 20X magnification at 48 hr. Decreased magnification at 48 hours was needed to maintain the larger nematodes in the field of view but all other optical parameters were held constant. Regions of interest were drawn around images of the nematodes acquired using differential interference contrast (DIC) imaging, and overlaid with fluorescence images obtained using a GFP filter set. The mean pixel intensities for GFP fluorescence were calculated and controls and treatments were compared using *t*-tests (α = 0.05). Image analysis was performed using the NIS-Elements software package (Nikon).

2.5.5 *Redox marker verification by immunoprecipitation*. Immunoprecipitation was performed with 100 µg of *C. elegans* protein, and immunoprecipitation and western blotting validation were performed following methods from a previously described protocol (Triplett et al., 2015). Antibodies that were used for redox verification included anti-PMT-2 (Abmart, Shanghai, China) (200 μg/mL; 1:600 dilution) and anti-ATP-2(WP:CE29950 generated using Genomic Antibody Technology at Strategic Diagnostics

Inc.) (SDI, Newark, DE). Data were tested using Bonferroni corrected t-tests with $\alpha =$ 0.10. We accepted a higher probability of a type one error for this tests because we could only perform a small number of replicates.

3. Results

3.1 CeO$_2$ nanomaterial characterization. TEM (SI Fig. 1) indicated that all CeO$_2$-ENMs had similar primary particle sizes (3.36 ± 0.80 nm for DEX-CeO$_2$, 3.88 ± 0.90 nm for CM-CeO$_2$, and 3.99 ± 0.71 nm for DEAE-CeO$_2$). The Z-average (intensity weighted) diameters from DLS were 15.69 nm for DEX-CeO$_2$, 8.72 nm for CM-CeO$_2$, and 13.54 nm for DEAE-CeO$_2$. Because Z-avearge diameters are intensity weighted, these small differences are not that significant. They could be a result of small differences in aggregation state or confirmation of the polymer on the surface. PALS analysis confirmed that each particle type had distinct neutral, negative, and positive charges in the exposure media (mean zeta potential of 2.27 mV for DEX-CeO$_2$, -22.2 mV for CM-CeO$_2$, and +27 mV for DEAE-CeO$_2$).

3.2 Caenorhabditis elegans mortality. None of the CeO$_2$-ENM treatments caused more than 50% mortality at the concentrations tested in L3 nematodes in the absence of food after a 24-hour exposure. DEAE-CeO$_2$ caused the highest mortality at all tested concentrations compared to CM-CeO$_2$ and DEX-CeO$_2$ nanomaterials (SI Fig. 2A). The addition of food resulted in slightly increased mortality in DEX-CeO$_2$ and DEAE-CeO$_2$ at 1,000 mg/L, but not in CM-CeO$_2$ exposures. Most notably, mortality of *C. elegans* in 5,000 mg/L DEAE-CeO$_2$ 24 hour fed exposures was 80% $\pm$ 10%. This is in contrast to mortality in CM-CeO$_2$ ($16.4\% \pm 5\%$) and DEX-CeO$_2$ ($25 \pm 6\%$,) (SI Fig. 2B).

3.3 Reproduction. All three CeO_2-ENM treatments reduced the number of nematode offspring compared to the control at the tested concentrations in a concentration-dependent manner. Control nematodes produced 168 ± 32 offspring (mean $\pm$ standard deviation). Nematodes exposed to DEX-CeO_2/L nanomaterials fewer offspring compared to controls at concentrations greater than 600 mg Ce/L ($p < 0.05$). Reproduction in CM-CeO_2 exposed nematodes was significantly reduced at a concentration of 1,000 mg/L (87 $\pm$ 77 offspring), and reproduction in CeO_2-DEAE exposed nematodes was only significantly reduced at 3.25 mg/L (87 ± 49 offspring) (Fig. 1). The EC_{30} values for reproduction for DEAE-CeO_2 were two orders of magnitude lower (3.25 mg/L) than to CM-CeO_2 (650 mg/L) and DEX-CeO_2 (500 mg/L).

3.4 Protein expression and oxidative proteomics

3.4.1 Immunochemical slot blots. The LC_{30} concentrations derived from the L2 mortality experiments were used to investigate the impacts of CeO_2-ENM exposure on oxidative and nitrosative stress in sublethal exposures. There was a marginally significant decrease in HNE levels for the DEAE-CeO_2 treatment compared to controls ($p = 0.106$). DEX-CeO_2 and CM-CeO_2 had no significant effect on HNE levels ($p = 0.411$). Protein carbonyls and 3NT levels were not significantly different from controls for all three treatments ($p = 0.733$) (SI Fig. 3).

3.4.2 Protein Expression Table 1 lists a summary of all proteins that were differentially expressed compared to controls. Table 1 columns are for spot numbers, fold change, *p*-value, and orbitrap MS-MS analysis (Swissprot accession number, percent of protein sequence covered by matching peptides, the number of peptide sequences that were identified by orbitrap-MS/MS, the confidence score, and the expected molecular weight

and isoelectric point of the identified protein). Figure 2A-D shows representative examples of SYPRO ruby stained gels generated from control, DEX-CeO$_2$, CM-CeO$_2$, and DEAE-CeO$_2$ treated nematodes protein. Twenty proteins exhibited significantly altered expression compared to controls. The ten proteins from DEX-CeO$_2$ protein gels that exhibited significantly altered expression compared to controls include myosin light chain 3 (MLC-3), pyruvate dehydrogenase (PDHB-1), superoxide dismutase (SOD-1), transketolase (TKT-1), peroxidreductase (PRDX-1), aldehyde dehydrogenase (ALH-12), heat-shock-related 70 kDa protein 1 (HSP70a; product of *hsp-1*) and protein 6 (HSP-70f; product of *hsp-6*), elongation factor (EEF-2), and paramyosin (UNC-15). The four proteins from CM-CeO$_2$ that exhibited significantly altered expression compared to control gels include probable s-adenosylmethionene synthase (SAMS-1), enolase (ENOL-1), paramyosin (UNC-15), and putative aminopeptidase (LAP-2). The six proteins from DEAE-CeO$_2$ that exhibited significantly altered expression compared to control gels include glyceraldehyde-3-phosphate dehydrogenase (GAPDH), v-type proton ATPase (VHA-12), enolase (ENOL-1), seryl amino acyl tRNA synthase (SARS-1), glutamate dehydrogenase (GDH-1), and leucine aminopeptidase (LAP-2).

3.4.3 Western blotting and detection of protein carbonyl, 3NT, and HNE Table 2 lists a summary of proteins that exhibited significantly altered oxidative and nitrosative modifications compared to control proteins. The columns in table 2 correspond to the columns described in supplementary table 1. Figure 3 shows representative 3NT western blots generated from control (Fig. 3A), DEX-CeO$_2$ (Fig. 3B), and CM-CeO$_2$ (Fig. 3C) treated nematode protein. Actin 5 (ACT-5) from DEX-CeO$_2$ blots and calreticulin (CRT-1), aspartic protease (ASP-5), phosphoethanolamine-N-methyltransferase (PMT-2),

adenosylhomocysteinase (AHCY-1), galectin (LEC-6), and nucleoside diphosphate kinase (NKD-1) from CM-CeO$_2$ blots exhibited significantly increased 3NT markers. Only two proteins, ATP synthase beta (ATP2) and glyceraldehyde-3-phosphate dehydrogenase (GAPDH), from CM-CeO$_2$ exhibited significant increases in protein carbonyls compared to controls. No proteins from DEAE-CeO$_2$ treatments exhibited significant changes in HNE, 3NT or protein carbonyls.

3.5 Validation Experiments

3.5.1 1D protein validation: Protein expression analysis in PDQuest indicated a 1.6-fold decrease in the expression of PDHB-1 after DEX-CeO$_2$ exposure ($p < 0.05$). One-dimensional gel verification indicated a 1.35-fold decrease in PDHB-1 expression in DEX-CeO$_2$ treatments ($p = 0.071$). Supplementary figure 4 shows the PDHB-1 western blot aligned with the total protein gel image for replicates 1-3 (control lanes 1, 5, and 9; DEX-CeO$_2$ in lanes 2, 6, and 10) (SI Fig. 4A) and replicates 4-6 (control lanes 1, 5, and 9, DEX-CeO$_2$ in lanes 2, 6, and 10) (SI Fig. 4B). These findings confirmed the down-regulation of PDHB-1 in *C. elegans* after exposure to DEX-CeO$_2$.

3.5.2 qRT-PCR: Protein expression analysis in PDQuest indicated a significant down-regulation at 2.62 and 2.77 fold change in the protein expression of HSP70a and HSP70f, respectively. The genes encoding these two proteins,*hsp-1* (gene for HSP70a protein) and *hsp-6* (gene for HSP70f protein), were analyzed by qRT-PCR using four independent replicates. Expression of *hsp-1* was down-regulated by 1.38-fold ($p = 0.001$) and expression of *hsp-6* was down-regulated by 1.73-fold ($p = 0.02$). These data are supportive of the down-regulated expression of HSP70a and HSP70f in *C. elegans* after

exposure to DEX-CeO$_2$. Protein expression analysis in PDQuest indicated a significant increase in the expression of ENOL-1 (increase of 1.97-fold) in CM-CeO$_2$ treatments (1.97-fold change, $p = 0.01$) and DEAE-CeO$_2$ treatments (2.23 fold change, $p = 0.01$). There was also up-regulation of *enol-1* observed in CM- and DEAE-CeO$_2$ treatments via aRT-PCR (1.52 and 1.09-fold change, respectively), but this was not statistically significant (SI Fig. 5).

3.5.3 Mutant reproduction assay: Protein expression analysis in PDQuest indicated a significant down-regulation of UNC-15 in DEX-CeO$_2$ (-2.94 fold change and $p = 0.025$) and CM-CeO$_2$ treatments (-333 fold change and $p = 0.003$). Results from the *unc-15* mutant reproduction assay indicated a 26% reduction in reproduction in mutant nematodes exposed to DEX-CeO$_2$ compared to N2 (wild-type) nematodes exposed to DEX-CeO$_2$ ($p = 0.06$). A 62% reduction in reproduction was also observed in *unc-15* mutant nematodes exposed to CM-CeO$_2$ compared to N2 nematodes exposed to CM-CeO$_2$ ($p = 0.007$). These data are supportive of the down-regulation of the UNC-15 protein observed in *C. elegans* after exposure to DEX- and CM-CeO$_2$ (SI Fig. 6).

3.5.4 GFP Fluorescence expression assay: Protein expression analysis in PDQuest indicated a significant down-regulation in HSP70f (predicted protein from *hsp-6* gene (Heschl and Baillie, 1990)) in *C. elegans* after exposure to DEX-CeO$_2$. In addition to validation by qRT-PCR (section 3.5.2), we investigated the reduction in HSP70f expression using a GFP reporter strain (*gfp*::*hsp-6*). GFP fluorescence was found to be significantly decreased at 24 hours post-exposure (reduction of 15%, $p = 0.003$), but this effect was not observed at 48 hours post-exposure (increase of 8%, $p = 0.35$). These data

are supportive of the down-regulation of HSP70f in *C. elegans* after exposure to DEX-CeO_2 (Fig. S7).

3.5.5 Redox verification by immunoprecipitation To validate the changes that were observed regarding protein carbonyls and 3NT, immunoprecipitation was performed on two proteins of interest, PMT-2 and ATP-2. (increased 3NT observed for PMT-2 proteins after CM-CeO_2 exposure and elevated protein carbonyls observed on ATP2 proteins after CM-CeO_2 exposure). Results indicated increased 3NT for PMT-2, but this was not statistically significant. Increased protein carbonyls were observed on ATP-2, but this was also not statistically significant. Due to a limited amount of protein available for these assays, only a small number of replicates could be performed, limiting statistical power. These fact that both assays indicated changes in the same direction as the 2-D gels is supportive of increased 3NT and protein carbonyls observed in PMT-2 and ATP-2, respectively (Fig S8).

4. Discussion

This study investigated the differential toxicity of three CeO_2-ENM particle types that specifically vary in surface charge conferred by addition of different functional groups to dextran coatings. Our findings indicate that surface chemistry is an important factor that influences CeO_2-ENM toxicity, where positively charged CeO_2-ENMs induce greater mortality and reproductive toxicity compared to neutral and negatively charged particles at similar concentrations. These data also indicate different modes of toxicity for the three differentially charged CeO_2-ENMs that were investigated. These results highlight that CeO_2-ENM toxicity can vary greatly among particle types, and that surface chemistry and charge are important characteristics that influence both the extent and

21

nature of CeO_2-ENM toxicity. Toxicity of CeO_2 to C. elegans has occurred over a wide range; however, effects of bare particles are generally seen at concentraitons around 1 mg/L (Collin et al., 2014a). That suggests that the DEAE coated particles are similar in toxicity to bare particles. The pH of zero net charge of ceria is around 7.6, so bare particles would be positively charged below this pH value (Gulicovski et al., 2014). Few studies have systematically compared size, although Roh et al., (2013), showed that nano CeO_2 is more toxic than micron-sized CeO_2 in *C. elegans*. The particles in the present study are among the smallest particles which have been studied for toxicity to date. We are not aware of studies that systematically compare shape either. Our results taken together with those of Zhang et al., (2011) and Asati et al., (2010), indicate that surface chemistry is the major determinant of toxicity within the nano size range.

It is important to keep in mind throughout the discussion that animals used for proteomics and other tests were exposed at equitoxic concentraitons, the EC30 for reproduction, therefore differences truly reflect differences in mechanism of toxicity, not in degree of toxicity. It is also important to keep in mind that we previously tested the toxicity of the free coatings and found no effects on reproduction or mortality at the highest concentrations at which they could occur as free polymer in the present study (Collin et al., 2014b).

4.1 Proteomic responses associated with cationic CeO_2-ENM toxicity

Cationic CeO_2-ENMs increased *C. elegans* mortality and decreased reproduction at concentrations that were one and two orders of magnitude lower than anionic or neutral

CeO$_2$-ENMs, indicating a higher potential for toxicity of ceria nanomaterials with cationic surface charges. The toxicity of cationic nanomaterials has been previously linked to elevated bioaccumulation in cells compared with neutral or negative particle types, and this is related to increased biological activity and toxicity of cationic nanomaterials (Frohlich, 2012). Previous work in our laboratory agrees with this, as the accumulation of Ce in *C. elegans* exposed to DEAE-CeO$_2$ was far greater than the accumulation of Ce in *C. elegans* exposed to DEX- and CM-CeO$_2$ when exposed at equivalent mass concentrations of Ce (Collin et al., 2014b).

Toxicity related to cationic nanomaterials could also be related to specific localization of particles to subcellular compartments. Further investigation of ceria bioaccumulation in *C. elegans* in our laboratory revealed a smaller reduction of Ce from Ce(IV) to Ce(III) after uptake of positively charged DEAE-CeO$_2$ by nematodes compared to uptake of DEX- and CM-CeO$_2$ (Collin et al., 2014b). We hypothesized that these differences in Ce speciation may be due to differences in the subcellular distribution of the particles, resulting in redox activity that is specific to the chemical conditions of those subcellular compartments. Cationic CeO$_2$-ENMs can localize to endosomes and lysosomes (Frohlich, 2012). Our own data support this, as we observed an increase in the protein expression of VHA-12 in *C. elegans* after exposure to DEAE-CeO$_2$. VHA-12 is subunit of a vacuolar proton pump that mediates acidification of endosomes, which eventually mature to become lysosomes to aid in degradation of foreign material taken into the cell by endocytosis (Syntichaki et al., 2005). Increased protein expression of VHA-12 is indicative of endosome acidification, and this could signify an attempt of the cell to degrade the DEAE-CeO$_2$ particles localized within the endosomes.

23

Results from expression proteomics indicate the exposure of *C. elegans* to DEAE-CeO$_2$ changed the expression of proteins related to carbohydrate metabolism. Enolase (ENOL-1) expression was increased and glyceraldehyde-3-phosphate dehydrogenase (GAPDH) and glutamate dehydrogenase (GDH-1) expression were decreased in nematodes exposed to DEAE-CeO$_2$. ENOL-1 and GAPDH are proteins with an important role in glycolysis. GAPDH is considered to be a housekeeping gene for genomics and proteomics assays, but these results indicate that GAPDH is not an appropriate reference gene for CeO$_2$-ENM toxicity assays. In addition, there is mounting evidence that GAPDH has multiple roles in the cell in addition to metabolism (Chuang et al., 2005), and decreases in GAPDH could reflect changes to these other biochemical pathways. GDH-1 is a mitochondrial enzyme that is important in the urea cycle, and GDH-1 creates a link between amino acid and carbohydrate metabolism in eukaryotic cells, including the nematode. It could indicate an increase in amino acid catabolism for energy production since it produces α-ketoglutarate, which can be used in the citric acid cycle to produce ATP. GDH-1 has been previously shown to be down-regulated in *Daphnia* after exposure to ZnO nanoparticles (Poynton et al., 2011).

Exposure of *C. elegans* to DEAE-CeO$_2$ decreased the expression of probable serine-tRNA synthetase (SARS-1) and increased the expression of putative aminopeptidase (LAP-2), indicating an impact of DEAE-CeO$_2$ on protein synthesis and degradation. LAP-2 is a cytosolic leucine aminopeptidase that degrades amines by catalyzing the hydrolysis of leucine residues at the N-terminus of proteins. The sequence of LAP-2 overlaps with LAP-1, which has been linked to digestive processes in *C. elegans* (Joshua, 2001). Increased expression of LAP-2 in *C. elegans* suggests that

DEAE-CeO$_2$ exposure might increase proteolytic activity in the *C. elegans* gut. Leucine aminopeptidase also belongs to the M17 family of metallopeptidases (Himmelhoch, 1969; Joshua, 2001), and increased expression of LAP-2 could point to increased metallo-enzymatic activity after exposure of *C. elegans* to DEAE-CeO$_2$.

Take together, it appears as though alteration in digestion and metabolism may be a major mechanism of DEAE-CeO2 toxicity. This could be the result of the particles accumulating on the intestinal epitheium causing damage. This would result in decreased nutrient assimilation effeciency and/or starvation as evidenced by a shift from glycolysis to oxidative phosphorylation and shift away from amino acid synthesis to proteolysis.

4.2 Proteomic responses associated with anionic CeO$_2$-ENM toxicity

Exposure of *C. elegans* to anionic CM-CeO$_2$ resulted in changes to two proteins (increase in ENOL-1 and decrease in LAP-2) that paralleled changes induced by DEAE-CeO$_2$. This indicates the potential for some similarity regarding mechanisms of toxicity between positively and negatively charged CeO$_2$-ENM particle types. Specifically, CM-CeO$_2$ and DEAE-CeO$_2$ might both have an impact on digestive processes, suggesting damage to the intestines.

While these similarities exist, there were also differences in the protein expression patterns. Exposure of *C. elegans* to anionic CM-CeO$_2$ resulted in a down-regulation of SAMS-1, and this is unique to the CM-CeO$_2$ treatment. SAMS-1 is a universal methyl donor for methyltransferase reactions that are important for lipid metabolism, and SAMS-1 is important for methylation of DNA, RNA, and protein (Li et al., 2011). SAMS-1 was

25

downregulated in $CM-CeO_2$ nematodes, and this could result in increased lipid droplet size in *C. elegans* (Li et al., 2011). SAMS-1 is also involved in one carbon metabolism, where nutrients from diverse sources (glucose, serine, threonine, methionine, and choline) are integrated to produce energy for various biological functions (Mentch and Locasale, 2016). Decreased expression of SAMS-1 could indicate that $CM-CeO_2$ disrupts digestive processes in the nematode. Downregulation of SAMS-1 could also result in changes to methylation patterns of the nematode epigenome. A recent study indicated that unlike mammals, which methylate cytosine, *C. elegans* methylates adenine (Greer et al., 2015). We recently conducted a multi-generational study of Ag nanoparticle toxicity in *C. elegans* that showed increased reproductive sensitivity in 2nd generation that persisted over eight generations suggesting strong evidence for epimutations (Schultz et al., 2016). In addition, decreased expression of UNC-15, a paramyosin homolog (Kagawa and Genyo, 1989), indicates that $CM-CeO_2$ exposure might disrupt the organization of muscle in the nematode body wall.

4.3 Mechanisms of neutral CeO_2-ENM toxicity

Protein expression profiles from nematodes treated with $DEX-CeO_2$ indicated a unique toxicity pathway for $DEX-CeO_2$ compared with CM- and $DEAE-CeO_2$. Both TKT-1 and PDBH-1 are thiamine dependent enzymes that require thiamine pyrophosphate (TPP) as cofactors for functional biological activity, and their expression was decreased in nematodes exposed to $DEX-CeO_2$. TKT-1 links the pentose phosphate pathway with glycolysis by channeling sugar phosphates to glycolysis (Coy et al., 1996) and PDHB-1 links glycolysis in the cytoplasm with oxidative phosphorylation in the

mitochondrion (Stacpoole, 2012). Cerium oxide has been shown to oxidize thiamine in acidic environments (Byadagi et al., 2010), and oxidized thiamine derivatives can interact with cell machinery and affect various cellular processes and metabolism (Parkhomenko et al., 1999). It is possible that our results indicate a disruption of metabolic processes in *C. elegans* that are linked with thiamine metabolism and oxidized thiamine derivatives.

Decreased expression of ALH-1 and EEF-2 was observed in nematodes exposed to DEX-CeO$_2$. ALH-1 is a mitochondrial protein that oxidizes aldehydes to carboxylic acids for aldehyde metabolism, and this activity is part of the biological detoxification process (Vasiliou et al., 2000). EEF-2 is important in the elongation phase of protein synthesis, and it is required for embryogenesis and vulval morphogenesis (Wong et al., 2016). Protein synthesis is energetically costly, and reductions to protein synthesis and metabolic activity have been linked with increased lifespan and stress resistance due to decrease in toxic metabolic byproducts and increased energy savings that can be re-allocated to cellular maintenance and repair (Hansen et al., 2007). In addition, many of the proteins that were down-regulated in DEX-CeO$_2$ treatments (TKT-1, EEF-2, HSP70) have roles in synthesis and maintenance of lipid droplets that can increase and decrease fat accumulation for energy storage (Vrablik et al., 2015).

DEX-CeO$_2$ also reduced expression of two structure-related proteins with roles in thick and heavy chain filaments (UNC-15) and light chain filaments (MLC-3), indicating that DEX-CeO$_2$ might disrupt cytoskeletal and muscle filament organization (Ben-Zvi et al., 2009). UNC-15 was also down-regulated in CM-CeO$_2$ treatments, indicating that both DEX- and CM-CeO$_2$ might induce toxicity by mechanisms that alter cellular structure.

A decrease in the expression of proteins that are important for the stress response was observed in *C. elegans* exposed to DEX-CeO$_2$. Expression of Cu/Zn superoxide dismutase (SOD1) protein was decreased in DEX-CeO$_2$ treatments, and expression of two proteins from the HSP70 family (HSP70A predicted from *hsp-1* gene and HSP70f predicted from *hsp-6* gene)(Heschl and Baillie, 1990) were decreased by DEX-CeO$_2$ treatments. Oxidative stress typically induces the expression of antioxidant and heat shock genes (Park et al., 2009) and proteins (Gupta et al., 2007), and the reduced expression of SOD1, HSP70a and HSP70f suggests that oxidative stress does not play a large role in the stress response of *C. elegans* to DEX-CeO$_2$. HSP70f is a protein importer localized to the mitochondria involved in mitochondrial biosynthesis and regulation of lifespan (Kimura et al., 2007). It is a homologue of human mortalin (mthsp70), which has been shown to reduce accumulation of ROS when overexpressed in PC12 cells (Liu et al., 2005). Furthermore, DEX-CeO$_2$ has been shown to act as a radical scavenger and antioxidant in other biological systems (Alili et al., 2011; Perez et al., 2008), and these results support the antioxidant nature of this particle type.

4.4 Oxidative damage to proteins by CeO$_2$-ENMs

Exposure of nematodes to CM-CeO$_2$ resulted in oxidative damage to the largest number of proteins (eight proteins) compared to DEAE- (no proteins) and DEX-CeO$_2$ (one protein). Increased 3NT residues, indicative of nitrosative damage, were found on CRT-1, ASP-5, PMT-2, AHCY-1, LEC-6, and NDK-1. Interestingly, two of these proteins are expressed in the nematode intestine (ASP-5 and LEC-6), and two of these proteins are involved in one carbon metabolism (PMT-2 and AHCY-1) (Martin et al.,

2011). Taken together, these data indicate that CM-CeO$_2$ could oxidize proteins in the intestine and subsequently influence digestive processes and metabolic pathways.

Only one protein, ACT-5, exhibited nitrosative damage after exposure to CeO$_2$-DEX. ACT-5 function is essential for the morphogenesis of intestinal microvilli (MacQueen et al., 2005), and it is possible that DEX-CeO$_2$ perturbs microvilli development in the nematode gut by formation of 3NT residues on ACT-5. Interestingly, in our previous study, the exposure of *C. elegans* to gold nanoparticles resulted in the up-regulation of the *act-5* gene, and these particles were also detected with TEM in the microvilli (Tsyusko et al., 2012).

Slot blot proteomics methods indicated no significant changes to global measures of oxidative stress. Although 2D-PAGE data indicate significant increases in protein carbonyls and 3NT oxidative measures, the lack of changes to global measures of oxidative stress suggests that other mechanisms of toxicity are also likely to be important in ceria nanomaterial toxicity.

4.5 conclusions

In summary, CeO$_2$-ENMs induced toxicity to *C. elegans*, and the level and mechanism of toxicity depended upon the surface charge of the particles. DEAE-CeO$_2$ was more toxic, but similarities in protein expression between DEAE- and CM-CeO$_2$ indicate similar mechanisms of toxicity for these particle types. The protein expression data showed that DEX-CeO$_2$ toxicity does not act solely by oxidative mechanisms, and that DEX-CeO$_2$ could disrupt fat and thiamine metabolism. According to protein expression and redox proteomics results, oxidative stress appears to be a more significant

player in CM-CeO$_2$ toxicity. CM-CeO$_2$ exposure also induced changes to protein expression and protein oxidative state of a number of proteins that play a role in one carbon metabolism. DEAE-CeO$_2$ exposure indicated changes to lysosomal activity and energy production. In addition, several proteins that exhibited altered expression across all the treatments were expressed primarily in the nematode gut, indicating that the gut is an important target that should be considered for CeO$_2$-ENM toxicity.

We previously hypothesized that toxicity of these materials in *C. elegans* was mediated through oxidation of macromolecules coupled with reduction of Ce in the CeO$_2$ structure from Ce IV to Ce III based X-ray absorption near edge spectroscopy (XANES)(Collin et al., 2014b). Furthermore, we hypothesized that differences in toxicity between coatings of different charge were primarily due to differences in the uptake and bioaccumulation of the particles, where the greatest bioaccumulation and toxicity occurred with positively charged particles. Studies using other positively charged coatings in *C. elegans* (HMT) also showed greatly enhanced toxicity in comparison to bare or negatively charged citrate coatings(Roh et al., 2010; Zhang et al., 2011). However, the data presented here, using the same materials and exposure scenario failed to provide convincing evidence that extensive oxidation of proteins occurred. It appears that the mechanism of nanoceria toxicity in *C. elegans* cannot be fully explained by oxidative stress mechanisms. While the preponderance of nanoceria toxicity research has focused on the oxidative stress mechanism, future studies should also consider alternative mechanisms of toxicity and the role of CeO$_2$ surface chemistry in those mechanisms. We provide evidence here that these materials may cause toxicity through a

number of different mechansims other than oxidative stress and they are highly dependent upon material surface chemistry.

Tables

Table 1. PD Quest and MS/MS results of *C. elegans* with significantly altered protein expression in treatments compared to controls.

Treatment	Spot ID	Protein	Accession #	MW	pI	Score	% Coverage	p-value	Fold Change
DEX-CeO$_2$	2003	**Myosin light chain 3 (MLC-3)**	**F09F7.2a**	**17.1**	**4.7**	**24**	**38**	**0.035**	**-2.44**
DEX-CeO$_2$	3327	**Pyruvate dehydrogenase (PDHB-1)**	**C04C3.3**	**38.1**	**6.01**	**51**	**24**	**0.005**	**-1.67**
DEX-CeO$_2$	5105	**Superoxide dismutase (SOD-1)**	**C15F1.7b**	**16.2**	**6.64**	**32**	**61**	**0.05**	**-1.56**
DEX-CeO$_2$	6707	**Transketolase (TKT-1)**	**F01G10.1**	**66**	**6.64**	**40**	**26**	**0.021**	**-1.61**
DEX-CeO$_2$	4107	**Peroxireductase (PRDX-1)**	**F09E5.15a**	**21.8**	**5.83**	**69**	**46**	**0.029**	**-1.89**
DEX-CeO$_2$	4602	**Aldehyde Dehydrogenase (ALH-12)**	**Y69F12A.2A**	**53.2**	**5.44**	**87.76**	**37.47**	**0.09**	**-2.13**
DEX-CeO$_2$	4705	**Heat Shock 70 kDa protein 1 (HSP70.1)**	**F26D10.3**	**69.7**	**5.64**	**154**	**48**	**0.002**	**-2.63**
DEX-CeO$_2$	4710	**Heat Shock 70 kDa protein 6 (HSP70.6)**	**C37H5.8**	**70.8**	**6.2**	**120**	**35**	**0.003**	**-2.78**
DEX-CeO$_2$	6820	**Elongation Factor 2 (EEF-2)**	**F25H5.4b**	**93.3**	**6.6**	**71.5**	**25**	**0.02**	**-2.13**
DEX-CeO$_2$	4805	**Parmyosin (UNC-15)**	**F07A5.7a**	**111.2**	**5.59**	**24**	**12.5**	**0.025**	**-2.94**
CM-CeO$_2$	5516	**Probable S-adenosylmethionene synthase (SAMS-1)**	**C49F5.1**	**43.6**	**6.48**	**43**	**28**	**0.007**	**-1.64**
CM-CeO$_2$	4509	**Enolase 1 (ENOL-1)**	**T21B10.2a**	**46.6**	**5.86**	**65**	**41**	**0.02**	**1.97**
CM-CeO$_2$	4805	**Paramyosin (UNC-15)**	**F07A5.7a**	**111.2**	**5.59**	**24**	**12.5**	**0.001**	**-333**
CM-CeO$_2$	7601	**Putative aminopeptidase (LAP-2)**	**W07G4.4**	**56.1**	**7.05**	**40**	**23**	**0.02**	**1.79**
DEAE-CeO$_2$	7408	**Glyceraldehyde 3 phosphate dehydrogenase (GAPDH)**	**K10B3.7**	**36.4**	**7.27**	**77**	**45**	**0.005**	**-1.45**
DEAE-CeO$_2$	3610	**V-type proton ATPase (VHA-12)**	**F20B6.2**	**54.7**	**5.48**	**98**	**45**	**0.038**	**1.61**
DEAE-CeO$_2$	4509	**Enolase 1 (ENOL-1)**	**T21B10.2a**	**46.6**	**5.86**	**65**	**41**	**0.012**	**2.23**
DEAE-CeO$_2$	5617	**Probable serine tRNA lidase (SARS-1)**	**C47E12.1**	**55.2**	**6.32**	**53**	**16**	**0.028**	**-2.04**
DEAE-CeO$_2$	6612	**Glutamate dehydrogenase (GDH-1)**	**ZK829.4**	**56.1**	**7.31**	**103**	**23**	**0.017**	**-1.47**
DEAE-CeO$_2$	7601	**Putative aminopeptidase (LAP-2)**	**W07G4.4**	**56.1**	**7.05**	**40**	**23**	**0.042**	**2.11**

Table 2: PDQuest and MS/MS results of *C. elegans* with significantly altered oxidative modifications (protein carbonyls, 3NT, HNE) compared to controls.

Treatment	Oxidative Mark	Spot ID	Protein	Accession #	MW	pI	Score	Coverage	p-value	Fold
DEX-CeO$_2$	3NT	4504	Actin 5 (ACT-5)	T25C8.2	41.8	5.68	86	43	0.03	28
CM-CeO$_2$	3NT	2601	Calreticulin (CRT-1)	Y38A10A.5	45.6	4.7	30	24	0.023	26
CM-CeO$_2$	3NT	3301	Aspartic protease 5 (ASP-5)	F21F8.3	42	6.06	51	14	0.007	9.86
CM-CeO$_2$	3NT	5502	Phosphoethanolamine N-methyltransferase (PMT-2)	F54D11.1	49.7	5.92	80	27	0.037	4.7
CM-CeO$_2$	3NT	5606	Adenosylhomocysteinase (AHCY-1)	K02F2.2	47.5	6.25	42	28	0.046	11.51
CM-CeO$_2$	3NT	6102	Galectin (LEC-6)	Y55B1AR.1	16	6.68	10.51	15.75	0.029	18.7
CM-CeO$_2$	3NT	7103	Nucleoside diphosphate kinase (NDK-1)	F25H2.5	17.1	7.5	13	26	0.034	25.7
CM-CeO$_2$	Protein carbonyl	4301	ATP synthase beta (ATP-2)	C34E10.6	57.5	5.77	122	51	0.04	-33.3
CM-CeO$_2$	Protein carbonyl	6208	Glyceraldehyde 3 phosphate dehydrogenase (GAPDH)	K10B3.7	36.4	7.27	48	21	0.005	-9

LEGEND

Table 1

PD Quest and MS/MS results of *C. elegans* with significantly altered protein expression in treatments compared to controls. Column 1 indicates the CeO_2 treatment associated with the sample; columns 2, 3, 4, 5, and 6 indicate spot ID, protein name, accession number, molecular weight (MW), isoelectric point (pI); column 7 and 8 indicate score and coverage of the identified protein, determined from MS-MS; and column 9 and 10 show the p-value and fold change of the associated proteins compared to control proteins, determined by analysis in PDQuest.

Table 2

PD Quest and MS/MS results of *C. elegans* with significantly altered oxidative/nitrosative marks in treatments compared to controls. Column 1 and 2 indicate CeO_2 treatment associated with the sample and the oxidative mark (protein carbonyl, 3NT, HNE) under investigation; columns 3, 4, 5, 6, and 7 indicate spot ID, protein name, accession number, molecular weight (MW), and isoelectric point (pI); columns 8 and 9 indicate score and coverage of the identified protein, determined from MS-MS; and columns 10 and 11 indicate the p-value and fold change of the associated protein compared to the control protein, determined by analysis in PDQuest.

Figure 1

Reproductive output of *C. elegans* calculated as total number of offspring per nematode after 48 hour exposure to DEX-CeO_2, CM-CeO_2, and DEAE-CeO_2. Asterisks indicate

34

reproduction is significantly different from controls (*p<0.05, **p<0.01, error bars indicate standard deviation).

Figure 2

Two-dimensional protein maps showing *C. elegans* protein expression after exposure to a) control, b) DEX-CeO$_2$, c) CM-CeO$_2$, and d) DEAE-CeO$_2$. Proteins were horizontally separated by isoelectric point from pH range 3 to 10, and vertically separated by molecular weight from 10 to 250 kDa. Marked proteins show a significant difference in spot density compared to control protein spot density. All significant spots are highlighted on the control gel. Spots are significant when $p < 0.05$.

Figure 3

Western blots of two dimensional protein gels from nematodes exposed to a) control, b) DEX-CeO$_2$, and c) CM-CeO$_2$, developed for the 3-nitrotyrosine (3NT) oxidative marker. Marked proteins exhibited significant changes in 3NT expression in the PDQuest program are highlighted on relevant blots. All significant spots are highlighted on the control blot. Spots are significant when $p < 0.05$.

References

Alili, L., Sack, M., Karakoti, A.S., Teuber, S., Puschmann, K., Hirst, S.M., Reilly, C.M., Zanger, K., Stahl, W., Das, S., Seal, S., Brenneisen, P., 2011. Combined cytotoxic and anti-invasive properties of redox-active nanoparticles in tumor-stroma interactions. Biomaterials 32, 2918-2929.

Asati, A., Santra, S., Kaittanis, C., Perez, J.M., 2010. Surface-Charge-Dependent Cell Localization and Cytotoxicity of Cerium Oxide Nanoparticles. Acs Nano 4, 5321-5331.

Ben-Zvi, A., Miller, E.A., Morimoto, R.I., 2009. Collapse of proteostasis represents an early molecular event in Caenorhabditis elegans aging. PNAS 106, 14914-14919.

Brenner, S., 1974. Genetics of Caenorhabditis elegans. Genetics 77, 71-94.

Byadagi, K.S., Naik, D.V., Savanur, A.P., Nandibewoor, S.T., Chimatadar, S.A., 2010. Ruthenium (III) mediated oxidation of thiamine hydrochloride by cerium (IV) in perchloric acid medium: a kinetic and mechanistic approach. Reac Kinet Mech Cat 99, 53-61.

Chen, J., Hessler, J.A., Putchakayala, K., Panama, B.K., Khan, D.P., Hong, S., Mullen, D.G., DiMaggio, S.C., Som, A., Tew, G.N., Lopatin, A.N., Baker, J.R., Jr., Holl, M.M.B., Orr, B.G., 2009. Cationic Nanoparticles Induce Nanoscale Disruption in Living Cell Plasma Membranes. Journal of Physical Chemistry B 113, 11179-11185.

Chigurupati, S., Mughal, M.R., Okun, E., Das, S., Kumar, A., McCaffery, M., Seal, S., Mattson, M.P., 2013. Effects of cerium oxide nanoparticles on the growth of keratinocytes, fibroblasts and vascular endothelial cells in cutaneous wound healing. Biomaterials 34, 2194-2201.

Choi, J., Tsyusko, O.V., Unrine, J.M., Chatterjee, N., Ahn, J.-M., Yang, X., Thornton, B.L., Ryde, I.T., Starnes, D., Meyer, J.N., 2014. A micro-sized model for the in vivo study of nanoparticle toxicity: what has *Caenorhabditis elegans* taught us? Environmental Chemistry 11, 227-246.

Chuang, D.M., Hough, C., Senatorov, V.V., 2005. Glyceraldehyde-3-phosphate dehydrogenase, apoptosis, and neurodegenerative diseases. Annu Rev Pharmacol Toxicol 45, 269-290.

Ciofani, G., Genchi, G.G., Mazzolai, B., Mattoli, V., 2014. Transcriptional profile of genes involved in oxidative stress and antioxidant defense in PC12 cells following treatment with cerium oxide nanoparticles. Biochim Biophys Acta 1840, 495-506.

Collin, B.; Auffan, M.; Johnson, A. C.; Kaur, I.; Keller, A. A.; Lazareva, A.; Lead, J. R.; Ma, X.; Merrifield, R. C.; Svendsen, C., 2014a. Environmental release, fate and ecotoxicological effects of manufactured ceria nanomaterials. Environmental Science: Nano 1, 33-548.

Collin, B., Oostveen, E., Tsyusko, O.V., Unrine, J.M., 2014b. Influence of Natural Organic Matter and Surface Charge on the Toxicity and Bioaccumulation of Functionalized Ceria Nanoparticles in *Caenorhabditis elegans*. Environmental Science & Technology 48, 1280-1289.

Costanzo, M.C., Hogan, J.D., Cusick, M.E., Davis, B.P., Fancher, A.M., Hodges, P.E., Kondu, P., Lengieza, C., Lew-Smith, J.E., Lingner, C., Roberg-Perez, K.J., Tillberg, M., Brooks, J.E., Garrels, J.I., 2000. The Yeast Proteome Database (YPD) and Caenorhabditis elegans Proteome Database (WormPD): comprehensive resources for the organization and comparison of model organism protein information. Nucleic Acids Research 28, 73-76.

Coy, J.F., Dubel, S., Kioschis, P., Thomas, K., Micklem, G., Delius, H., Poustka, A., 1996. Molecular cloning of tissue specific transcripts of a transketolase-related gene: Implications for the evolution of new vertebrate genes. Genomics 32, 309-316.

Donkin, S.G., Williams, P.L., 1995. Influence of developmental stage, salt, and food presence on various end-points using *Caenorhabditis elegans* for aquatic testing. Environmental Toxicology and Chemistry 14, 2139-2147.

Frohlich, E., 2012. The role of surface charge in cellular uptake and cytotoxicity of medical nanoparticles. Int J Nanomedicine 7, 5577-5591.

Goodman, C.M., McCusker, C.D., Yilmaz, T., Rotello, V.M., 2004. Toxicity of gold

nanoparticles functionalized with cationic and anionic side chains. Bioconjugate Chemistry 15,

897-900.

Greer, E.L., Blanco, M.A., Gu, L., Sendinc, E., Liu, J., Aristizabal-Corrales, D., Hsu, C.H.,

Aravind, L., He, C., Shi, Y., 2015. DNA Methylation on N6-Adenine in *C. elegans*. Cell 161,

868-878.

Gulicovski, J. J.; Bračko, I.; Milonjić, S. K., 2014. Morphology and the isoelectric point of

nanosized aqueous ceria sols. Mater Chem Phys 148, 868-873.

Gupta, S.C., Siddique, H.R., Mathur, N., Vishwakarma, A.L., Mishra, R.K., Saxena, D.K.,

Chowdhuri, D.K., 2007. Induction of hsp70, alterations in oxidative stress markers and apoptosis

against dichlorvos exposure in transgenic *Drosophilia melanogaster*: Modulation by reactive

oxygen species. Biochimica et Biophysica Acta 1770, 1382-1394.

Hansen, M., Taubert, S., Crawford, D., Libina, N., Lee, S.-J., Kenyon, C., 2007. Lifespan

extension by conditions that inhibit translation in *Caenorhabditis elegans*. Aging Cell 6, 95-110.

Hardas, S.S., Sultana, R., Warrier, G., Dan, M., Florence, R.L., Wu, P., Grulke, E.A., Tseng,

M.T., Unrine, J.M., Graham, U.M., 2012. Rat brain pro-oxidant effects of peripherally

administered 5nm ceria 30 days after exposure. Neurotoxicology 33, 1147-1155.

Heschl, M.F.P., Baillie, D., L., 1990. The HSP70 multigene family of *Caenorhabditis elegans*.

Comparative Biochemistry and Physiology 96b, 633-637.

Himmelhoch, S.R., 1969. Leucine Aminopeptidase: A Zinc Metalloenzyme. Archives of

Biochemistry and Biophysics 134, 597-602.

Joshua, G.W.P., 2001. Functional analysis of leucine aminopeptidase in *Caenorhabditis elegans*.

Molecular and Biochemical Parasitology 113, 223-232.

Kagawa, H., Genyo, K., 1989. Paramyosin gene (unc-15) of *Caenorhabditis elegans* molecular cloning, nucleotide sequence and models for thick filament structure. Journal of Molecular Biology 207, 311-333.

Kimura, K., Tanaka, N., Nakamura, N., Takano, S., Ohkuma, S., 2007. Knockdown of mitochondrial heat shock protein 70 promotes progeria-like phenotypes in *Caenorhabditis elegans*. The Journal of Biological Chemistry 282, 5910-5918.

Leung, M.C.K., Williams, P.L., Benedetto, A., Au, C., Helmcke, K.J., Aschner, M., Meyer, J.N., 2008. *Caenorhabditis elegans*: An emerging model in biomedical and environmental toxicology. Toxicological Sciences 106, 5-28.

Li, Y., Na, K., Lee, H.-J., Lee, E.-Y., Paik, Y.-K., 2011. Contribution of sams-1 and pmt-1 to lipid homeostasis in adult *Caenorhabditis elegans*. Journal of Biochemistry 149, 529-538.

Liu, Y., Liu, W., Song, X.D., Zuo, J., 2005. Effect of GRP75/mthsp70/PBP74/mortalin overexpression on intracellular ATP level, mitochondrial membrane potential and ROS accumulation following glucose deprivation in PC12 cells. Molecular and cellular biochemistry 268, 45-51.

MacQueen, A.J., Baggett, J.J., Perumov, N., Bauer, R.A., Januszewskit, T., Schriefer, L., Waddle, J.A., 2005. ACT-5 is an essential *Caenorhabditis elegans* actin required for intestinal microvilli formation. Molecular Biology of the Cell 16, 3247-3259.

Martin, F.-P.J., Spanier, B., Collino, S., Montoliu, I., Kolmeder, C., Giesbertz, P., Affolter, M., Kussmann, M., Daniel, H., Kochhar, S., Rezzi, S., 2011. Metabotyping of *Caenorhabditis elegans* and their culture media revealed unique metabolic phenotypes associated to amino acid deficiency and insulin-like signaling. Journal of Proteome Research 10, 990-1003.

Materials), A.A.S.f.T.a., 2012. Standard Terminology Relating to Nanotechnology (Active Standard ASTM E2456), Annul Book of ASTM Standard, Philadelphia, USA, 14.02.

Mentch, S.J., Locasale, J.W., 2016. One-carbon metabolism and epigenetics: understanding the specificity. Ann N Y Acad Sci 1363, 91-98.

Park, E.J., Choi, J., Park, Y.K., Park, K., 2008. Oxidative stress induced by cerium oxide nanoparticles in cultured BEAS-2B cells. Toxicology 245, 90-100.

Park, S.-K., Tedesco, P.M., Johnson, T.E., 2009. Oxidative stress and longevity in *C. elegans* as mediated by SKN-1. Aging Cell 8, 258-269.

Parkhomenko, I., Stepuro, I., Donchenko, G., Stepuro, V., 1999. Oxidized derivatives of thiamine: formation, properties, biological role. Ukr Biokhim Zh 84, 5-24.

Perez, J.M., Asati, A., Nath, S., Kaittanis, C., 2008. Synthesis of biocompatible dextran-coated nanoceria with pH-dependent antioxidant properties. Small 4, 552-556.

Pfaffl, M., Horgan, G.W., Dempfle, L., 2002. Relative expression software tool (REST) for group-wise comparison and statistical analysis of relative expression results in real-time PCR. Nucleic Acids Research 30, 1-10.

Pirmohamed, T., Dowding, J.M., Singh, S., Wasserman, B., Heckert, E., Karakoti, A.S., King, J.E.S., Seal, S., Self, W.T., 2010. Nanoceria exhibit redox state-dependent catalase mimetic activity. Chemical Communications 46, 2736-2738.

Poynton, H.C., Lazorchak, J.M., Impellitteri, C.A., Smith, M.E., Rogers, K., Patra, M., Hammer, K.A., Allen, J.H., Vulpe, C.D., 2011. Differential gene expression in *Daphnia magna* suggests distinct modes of action and bioavailability for ZnO nanoparticles and Zn ions. Environmental Science & Technology 45, 762-768.

Ranga, G., Mishra, B., 2003. Structural, redox and catalytic chemistry of ceria based materials. Bulletin of the Catalysis Society of India 2, 122-134.

Rogers, S., Rice, K.M., Manne, N.D., Shokuhfar, T., He, K., Selvaraj, V., Blough, E.R., 2015. Cerium oxide nanoparticle aggregates affect stress response and function in *Caenorhabditis elegans*. SAGE Open Med 3, 2050312115575387.

Roh, J.-Y., Park, Y.-K., Park, K., Choi, J., 2010. Ecotoxicological investigation of CeO_2 and TiO_2 nanoparticles on the soil nematode *Caenorhabditis elegans* using gene expression, growth, fertility, and survival as endpoints. Environmental Toxicology and Pharmacology 29, 167-172.

Schultz, C.L., Wamucho, A., Tsyusko, O.V., Unrine, J.M., Crossley, A., Svendsen, C., Spurgeon, D.J., 2016. Multigenerational exposure to silver ions and silver nanoparticles reveals heightened sensitivity and epigenetic memory in *Caenorhabditis elegans*. Proceedings of the Royal Society B: Biological Sciences 283.

U.S.EPA, 1998. Method 3015: Inductively Coupled Plasma Mass Spectrometry, United States Environmental Proteciton Agency, Washington, DC, USA.

Stacpoole, P.W., 2012. The pyruvate dehydrogenase complex as a therapeutic target for age-related diseases. Aging Cell 11, 371-377.

Steele, B.C.H., 1999. Fuel-cell technology - Running on natural gas. Nature 400, 619-+.

Steele, B.C.H., Heinzel, A., 2001. Materials for fuel-cell technologies. Nature 414, 345-352.

Sultana, R., Butterfield, D.A., 2008. Slot-blot analysis of 3-nitrotyrosine-modified brain proteins, in: E. Cadenas, L. Packer (Eds.), Nitric Oxide, Part F: Oxidative and Nitrosative Stress in Redox Regulation of Cell Signaling, 309-316.

Syntichaki, P., Samara, C., Tavernarakis, N., 2005. The vacuolar H+ -ATPase mediates intracellular acidification required for neurodegeneration in *C. elegans*. Curr Biol 15, 1249-1254.

Triplett, J.C., Zhang, Z., Sultana, R., Cai, J., Klein, J.B., Bueler, H., Butterfield, D.A., 2015. Quantitative expression proteomics and phosphoproteomics profile of brain from PINK1 knockout mice: insights into mechanisms of familial Parkinson's disease. Journal of Neurochemistry 133, 750-765.

Tsyusko, O.V., Unrine, J.M., Spurgeon, D., Blalock, E., Starnes, D., Tseng, M., Joice, G., Bertsch, P.M., 2012. Toxicogenomic responses of the model organism *Caenorhabditis elegans* to gold nanoparticles. Environ Sci Technol 46, 4115-4124.

USEPA, 2002. Methods for measuring the acute toxicity of effluents and receiving waters to freshwater and marine organisms (EPA-821-R-02-012), United States Environmental Protection Agency, Washington, D. C., USA.

Van Hoecke, K., Quik, J.T.K., Mankiewicz-Boczek, J., De Schamphelaere, K.A.C., Elsaesser, A., Van der Meeren, P., Barnes, C., McKerr, G., Howard, C.V., Van De Meent, D., Rydzynski, K., Dawson, K.A., Salvati, A., Lesniak, A., Lynch, I., Silversmit, G., De Samber, B., Vincze, L., Janssen, C.R., 2009. Fate and Effects of CeO2 Nanoparticles in Aquatic Ecotoxicity Tests. Environmental Science & Technology 43, 4537-4546.

Vasiliou, V., Pappa, A., Petersen, D.R., 2000. Role of aldehyde dehydrogenases in endogenous and xenobiotic metabolism. Chemico-Biological Interactions 129, 1-19.

Vrablik, T.L., Petyuk, E.M., Smith, R.D., Watts, J.L., 2015. Lipidomic and proteomic analysis of *Caenorhabditis elegans* lipid droplets and identification of ACS-4 as a lipid droplet-associated protein. Biochimica et Biophysica Acta 1851, 1337-1345.

Wang, B., Wu, P., Yokel, R.A., Grulke, E.A., 2012. Influence of surface charge on lysozyme adsorption to ceria nanoparticles. Applied Surface Science 258, 5332-5341.

Williams, P.L., Dusenbery, D.B., 1988. Using the nematode *Caenorhabditis elegans* to predict mammalian acute lethality to metallic salts. Toxicology and Industrial Health 4, 469-478.

Williams, P.L., Dusenbery, D.B., 1990. Aquatic Toxicity Testing Using the Nematode, *Caenorhabditis elegans*. Environmental Toxicology and Chemistry 9, 1285-1290.

Wong, R.-R., Kong, C., Lee, S.-H., Nathan, S., 2016. Detection of *Burkholderia pseudomallei* toxin-mediated inhibition of protein synthesis using a *Caenorhabditis elegans* ugt-29 biosensor. Scientific Reports Nature 6, 1-14.

Yokel, R.A., Florence, R.L., Unrine, J.M., Tseng, M.T., Graham, U.M., Wu, P., Grulke, E.A., Sultana, R., Hardas, S.S., Butterfield, D.A., 2009. Biodistribution and oxidative stress effects of a systemically-introduced commercial ceria engineered nanomaterial. Nanotoxicology 3, 234-248.

Zhang, H., He, X., Zhang, Z., Zhang, P., Li, Y., Ma, Y., Kuang, Y., Zhao, Y., Chai, Z., 2011. Nano-CeO$_2$ Exhibits Adverse Effects at Environmental Relevant Concentrations. Environmental Science & Technology 45, 3725-3730.

Zhang, Y., Chen, D., Smith, M.A., Zhang, B., Pan, X., 2012. Selection of reliable reference genes in *Caenorhabditis elegans* for analysis of nanotoxicity. PLoS One 7, e31849.
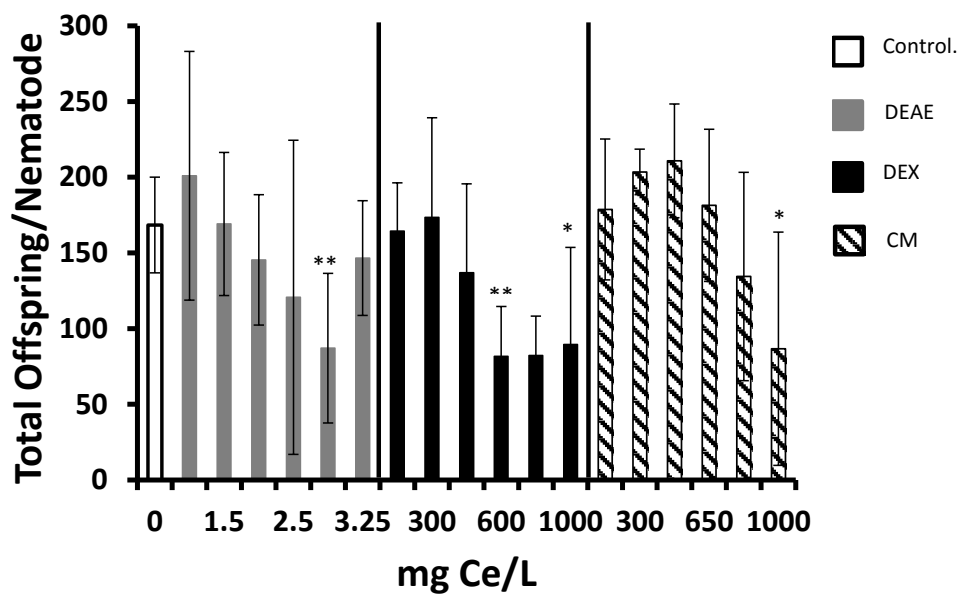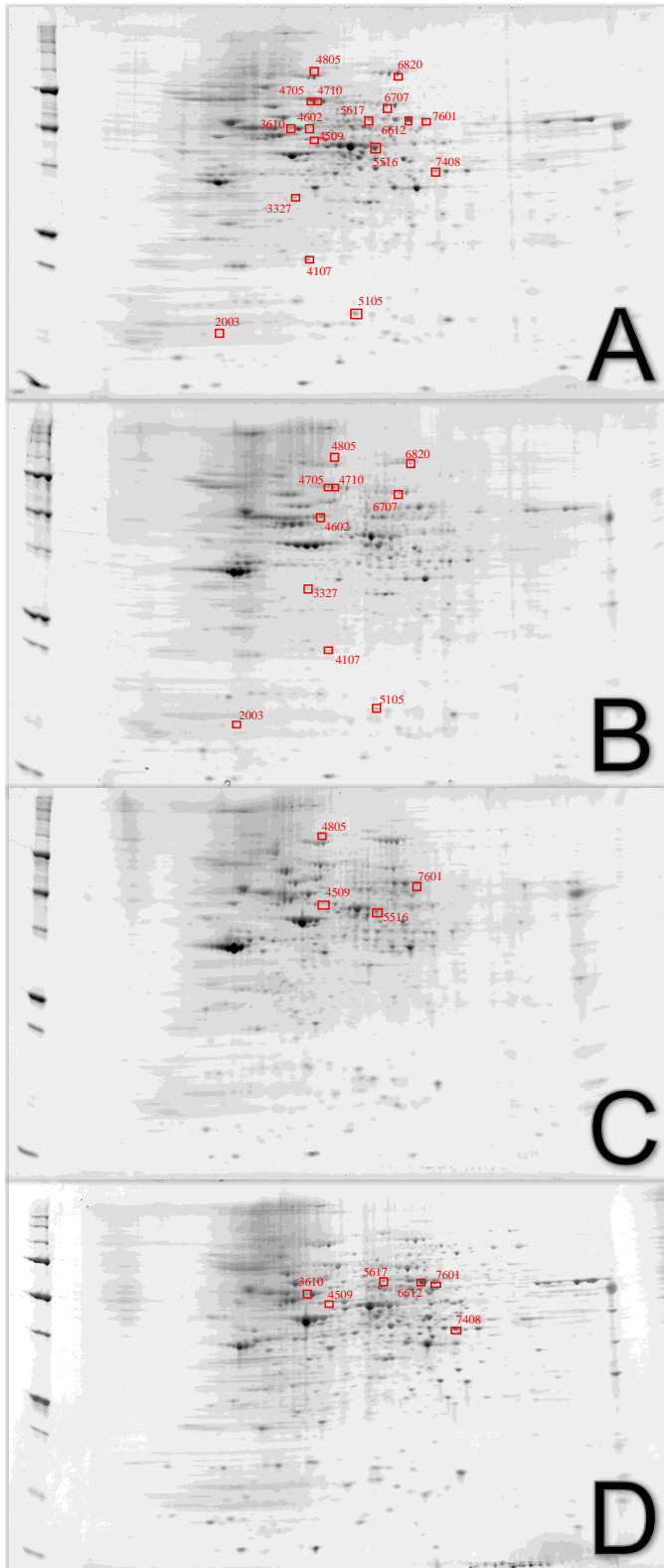
Figure 1

Figure 2

Figure 3